

Luminescence properties of por.Si–CdS/ZnS:Cu(Mn) nanostructured films

M. A. JAFAROV*, E. F. NASIROV, S. A. JAHANGIROVA
Baku State University, Baku, Azerbaijan

An aqueous solution method has been developed for synthesizing size-controlled Por.Si–CdS:Cu (Mn) and Por.Si–ZnS:Cu (Mn) nanocrystals with a relatively narrow size distribution. The nanocrystal samples were characterized by photoluminescence spectra. We prepared narrow size distribution particles under different synthesis conditions. The photoluminescence properties Por.Si-CdS:Cu (Mn) and Por.Si-ZnS:Cu (Mn) nanostructured films were investigated. Luminescence intensity in different excitation wavelength correlates with different size of CdS and ZnS nanocrystals on luminescence spectra. We found that by narrowing the size distribution and doping concentration, ZnS:Cu, Mn samples can be prepared with high luminescence intensity.

(Received February 6, 2019; accepted October 9, 2019)

Keywords: Aqueous solution, Nanoscale materials, Nanoparticles, Porous-Si, Luminescence

1. Introduction

Nanoscale materials researches have stimulated great interest owing to their importance in basic scientific research and potential technological applications. The synthesis of doped nanocrystals has become a major field of recent researches. ZnS:Cu, Mn nanocrystals have been mainly studied due to the luminescence of the Cu^{2+} and Mn^{2+} ions inside the CdS and ZnS host. This is due to the fact that Mn^{2+} ions provide good traps for the excited electrons, which give rise to their potential use in nonlinear optics, optoelectronic devices, solar cells, photodetectors and light-emitting diodes [1–3]. This paper presents some interesting results obtained on the synthesis of ZnS:Cu nanocrystals by the aqueous solution method with controllable and narrow size distribution. We treat the effect of Cu doping on the luminescence properties of ZnS nanoparticles. Also, we consider the effect of various synthesizing conditions on the narrow size distribution of the ZnS:Cu particles and the luminescence intensity.

Thin film heterojunctions of p(n)-Si/CdS are promising candidates for solar cell application [4, 5]. Since, application of wide-gap semiconductors as optical window in silicon-based heterojunctions, to some extent, allows minimizing the free charge losses due to surface recombination. However, significant difference in the lattice constants of silicon and CdS (about 7%) stimulates the formation of surface states at interface. Application of the solutions of A^2B^6 type semiconductors, as reported by us [6], has succeeded in reducing the lattice mismatch and concentration of surface states at interface, but it has not been possible to achieve sufficiently value of efficiency due to the large value of silicon refractive index. The use of porous silicon as an intermediate layer between the absorber and buffer, allows not only solving problems with lattice mismatches, and surface reflections related to refractive index of silicon, as reported by authors [8-10].

In this paper the photoluminescence properties Por.Si-CdS:Cu (Mn) and Por.Si-ZnS:Cu (Mn) nanostructured films were investigated.

2. Experimental

To manufacture the heterojunctions, p-type *c*-Si wafers (2.5 Ohm·cm resistivity and 0.2 ÷ 0.3 mm thickness) of (100) orientation were used as a substrate. Before anodization, the surface of the *c*-Si substrates were etched in an aqueous solution of HF and further washed in distilled water (at temperature of 80°C) and ethyl alcohol and then dried in air. The anodization of *c*-Si substrate surface was carried out in Teflon chamber with Pt cathode. HF: ethanol solution (1:1) were used for the porous silicon formation. The anodization voltage, current density and anodization time were 30V, 40-70 mA/cm² and 30–1800 sec, correspondingly. Depending on the anodization current and time porous-Si with porous size of 7 – 50 nm were prepared on the surface of *c*-Si.

In order to fabricate the heterojunctions, an ohmic In electrode, in reticulate form was evaporated on the CdS films with an area of ~0.82-1cm². An ohmic contact was performed on the side of *c*-Si wafers by evaporating an Al electrode.

Aqueous solutions of zinc chloride, copper chloride and the capping agent thioglycerol (TG) of high (0.1 and low (0.01 M) concentrations are prepared in ethanol. The pH was adjusted to about 2–10 by adding appropriate amounts of NaOH, before adding TG. Sodium sulfide dissolved in distilled water was added dropwise to the mixture for 5 min. The total reaction time was about 2 h. Nitrogen gas was used for deoxygenating the reaction vessel. The temperature in different experiments ranged between 30°C and 70°C. In high temperature experiments, the synthesis vessel was heated in the bath. The synthesis

solution was washed with acetone to get rid of unreacted ions remaining outside the clusters and then was centrifuged. Finally, the precipitate was air-dried to get a powder of ZnS:Cu, Mn nanoparticles. Deposited films were kept "as it were" for the other characterization like XRD and AFM. Thickness of the films was measured by gravity method. Thickness for CdS, ZnS:Cu, Mn films was varied from 84 – 85.26 nm. The luminescence spectra were recorded on a LF-5 Perkin Elmer spectrometer with the excitation wavelengths of about 370 nm to excite the ZnS:Cu, Mn nanocrystals.

3. Results

Fig. 1 shows the XRD patterns of CdS, ZnS CdS):Cu, (Mn) and, (ZnS):Cu, (Mn) thin films deposited at fixed pH value and temperature of 70°C. The XRD peaks appear at 33.20°, 47.32°, 56.36° and 69.4° in the pure ZnS film corresponding to the diffraction from (111), (220) and (311) planes respectively of the cubic phase ZnS. Results are very much closer to the value of JCPDS card file 05-0566. Same diffraction peaks are also observed in the ZnS:Cu films except in the 0.05M CuCl doped film (ZnS:Cu), where the (400) plane is absent. Thus all the deposited films are polycrystalline in nature. From the XRD spectra it is clear that the intensity of (220) plane in all the films higher than that of the other peaks which indicates that the orientation of the grain growth is along (220) plane.

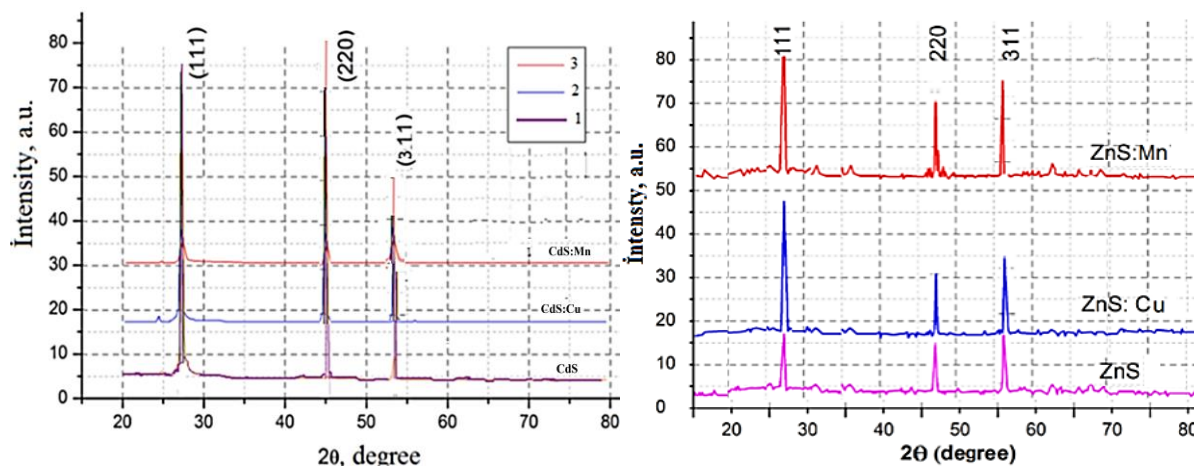


Fig. 1. XRD spectra of CdS:Cu, Mn: undoped nanocrystals (1), 3% Cu (2) and 3% Mn (3) doping nanocrystals and ZnS:Cu, Mn: undoped nanocrystals, 3% Cu and 3% Mn doping nanocrystals

Atomic force microscopy (AFM) is one of the effective ways for the surface analysis of thin films due to its high resolution and powerful analysis software.

The CdS and ZnS thin films were morphologically characterized using AFM technique.

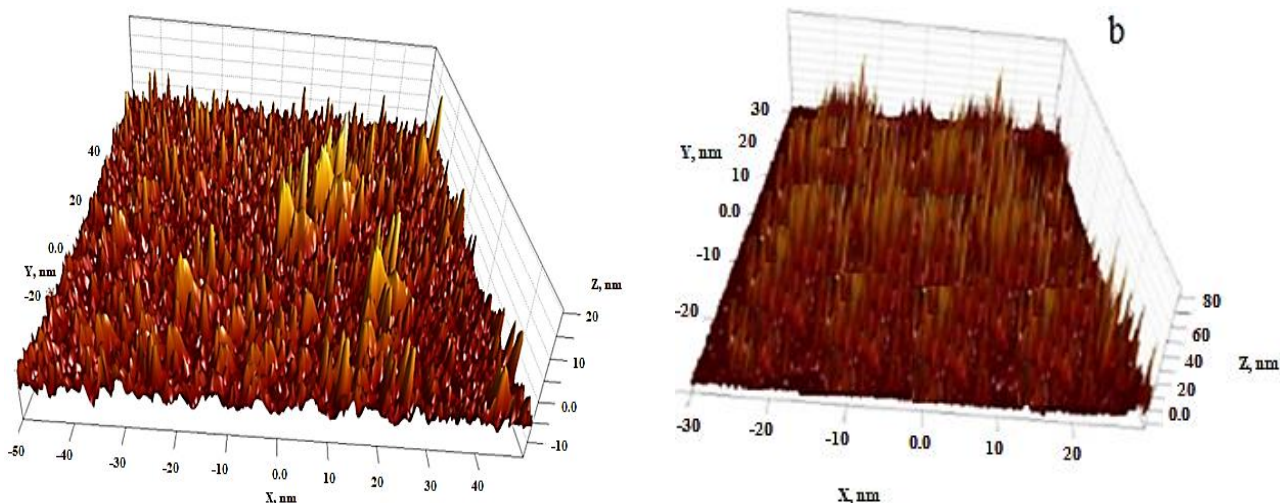


Fig. 2. AFM images of CdS(a) and ZnS: (b) films

Fig. 2 shows the image of CdS and ZnS film in scanned area of 5×5 and $10 \times 10 \mu\text{m}^2$. In both the films the surface is rough and fully covered in the substrate. Clusters of particles are observed over the surface in undoped ZnS film. While formation of different sizes are observed clearly with pinhole free in ZnS:Cu, Mn film correspond to band edge, shallow traps, and deep traps. Figs. 3 and 4 show the PL spectra of a series of Por.Si-CdS:Cu (Mn) and Por.Si-ZnS:Cu (Mn) nanostructured films.

These activities in the host material define the luminescence efficiency and can produce a narrowing or broadening of the bandwidth of the spectra. As shown in all figures, we have three peaks that can correspond to band edge, shallow traps, and deep traps. Figure 3 shows the PL spectra of CdS nanocrystals a series of samples. For a typical nanoparticle sample, luminescence can be generally divided into band edge emission, including excitonic emission, and trap state emission. The luminescence spectra of the ZnS nanocrystals are shown in Fig. 4.

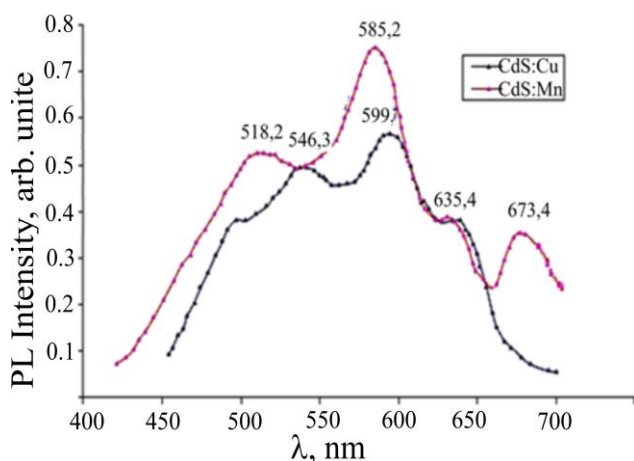


Fig. 3. Luminescence spectra of 3% Cu (1) and 3% Mn (2) doping CdS, nanocrystals

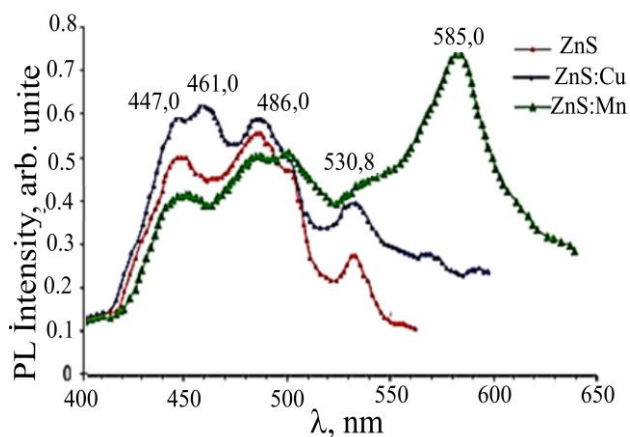


Fig. 4. Luminescence spectra of undoped ZnS nanocrystals (1), 3% Cu (2) and 3% Mn (3) doping ZnS nanocrystals

4. Discussions

It was found that the luminescence spectra for all samples could be deconvoluted into two individual components, which corresponded to band edge emission and surface trap state emission [6]. The mechanism of luminescence in CdS/ZnS nanostructure can be explained as following: after excitation, energy will be transferred from the conduction band of ZnS host to the excited charge carriers which are trapped in shallow trap states. These trapped charge carriers are followed by either energy transfer to the excited state of a Cu^+ ion, or radiative recombination with a deeply trapped hole at a defect state [7].

We explained the synthesis properties of ZnS:Cu samples. In contrast the trap states are located within the semiconductor band gap and hence their emission is usually red-shifted relative to the band edge emission. In addition, the trap state luminescence is often characterized by a large band width reflecting abroad energy distribution of the emitting states. Nonradiative decay pathways associated with unpassivated surface atoms competed with radiative exciton recombination.

The characteristic luminescence can consist of relatively sharp emission bands (spectral width typically a few nm), but also of broad bands, whose width can exceed 50 nm in the visible part of the spectrum. Sharp emission bands are characteristic of optical transitions between electronic states with chemical bonding character (almost) the same for ground and excited states that hardly participate in the chemical bonding. These activities in the host material define the luminescence efficiency and can produce a narrowing or broadening of the band width of the spectra.

The PL spectra (Fig. 3) of the nanocrystal samples show three peaks, at 518,2, 585,2, and 673,4 nm, which are attributed to the band edge, shallow and deep traps, respectively. We see that undoped nanocrystals have a narrower size distribution than the 3% doping CdS:Cu nanocrystals.

Therefore they have the highest emission intensity. But we expected doping Cu ions to produce better luminescence spectra. The impurity concentrations generally are low in view of the fact that at higher concentration the efficiency of the luminescence process usually decreases (concentration quenching). It may be that, at high concentration, there is the broad size distribution of nanocrystals and broad emission wavelength, and as a result, low luminescence intensity.

The nanocrystals of the A^2B^6 type compounds have high absorption intensities and photostability with a large absorption coefficient. The addition of these nanocrystals to the atoms of metals is one of the methods to obtain controllable materials with the spectrum of radiation in the required range. To this end, we investigated the luminescence properties of CdS and ZnS nanocrystals by Cu and Mn atoms.

During the synthesis of CdS, 3% CuCl_2 or MnCl_2 was added to the solution. CdS: The study of the luminescence

of Cu particles revealed that T2 levels of Cu atoms play an important role as an irradiation center. Thus, transition from the conductive zone and narrower donor level (sulfur vacancy) to T2 levels gives high intensity luminescence. The first maximum of the spectrum (546,3 nm) belongs to the donor-acceptor pair in the CdS crystal cage (Figure 3). The second maximum (599,7 nm) occurs when the Cu passes from T2 to the T2 level. The third maximum (635,4 nm) depends on the transition from the donor level to the additive level and partly weakens the luminescence line of the silica pores. CdS: The luminescence of the Mn particles is distinct and the main maximum is the high intensity of irradiation, even though it remains in the manganese CdS monocrystalline. The main maximum (585,2 nm) belongs to the mangle and it has been determined that the transversal irradiation recombination mechanism between the 4T1 to 6A1 intracellular levels of the mast is determined. The two maximum (518,2 nm and 673,4 nm) depend on the transition from donor levels to valent zones. The maximum silica pumps corresponding to 635,4 nm.

Semiconductor nanocrystals, known as light-emitting and quantum points, were widely studied in the last two decades. Their measurable optical properties, wide spectrum of excitations, narrow emission strips and high quantum efficiency, the light source in various optoelectric devices, the basic element of solar cells, environmental, rehabilitation, therapeutic and biological applications attract attention. Unfortunately, so far, commonly used compounds in many areas have been synthesized from toxic elements (such as Cd, Pb, Hg, Te, etc.) [3]. The main advantage of manganese-alloy ZnS nanocrystals compared with others is that they are resistant to temperature and environmental changes, with low toxicity, high survival time. ZnS is the most important semiconductor material of type flat zone with a large banned zone (3.7 eV). With its optical and optoelectronic properties, nano-dimensional ZnS draws attention. Considering these, we investigated the luminescence properties of both ZnS and pure copper

The first (447 nm) and third (486 nm) spectra of the spectrum relate to pure ZnS because the first is the transition from a donor level to a valence zone as the sulfur vacancy, and the latter to the transcriptional level (syndrome vaccine). The remaining two maximums are related to the transition level. ZnS:

The study of the luminescence of the Cu particles revealed that T2 levels of Cu atoms here play an important role as an irradiation center. Thus, transition from the conductive zone and the donor level (sulfur vacuum) to the T2 level gives high intensity luminescence. The second maximum (461 nm) occurs at the transition zone from Cu to T2. The third maximum (530,8 nm) depends on the transition from the donor level to the additive level. The intensity is the maximum (585 nm) mantle and is explained by the cross-sectional irradiation recombination mechanism between the center 4T1 to 6A1 levels.

5. Conclusions

It means that doping of nanocrystals occurs completely in high precursor concentration. Also, we investigated the optimize conditions for the best luminescence with different excitation wavelengths and doping concentrations there is a narrowing of the excitonic absorption peak at 350 nm. We excited sample K with three excitation wavelengths. There is the best luminescence for 360 nm excitation which is near to band edge wavelength. Two other excited emissions related to the sizes of other nanoparticles were distributed in this sample. We find a red-shift of the band edge emission by varying the excited wavelength. But we have abroad peak at 465 nm in all of them that is related to the incorporation of non radiative and radiative recombination.

References

- [1] A. Oliva, Applied Surface Science **205**(1-4), 56 (2003).
- [2] Ch. Kumar, Journal of the Korean Physical Society, **55**(1), 284 (2009).
- [3] C. Perkins, Journal of Vacuum Science and Technology A, Vacuum Surfaces and Films **24**(3), 497 (2006).
- [4] D. Patidar, Bull. Matt. Sci. **29**(1), 21 (2006).
- [5] M. Jafarov, International Journal of Scientific and Engineering Research **6**(7), 849 (2015).
- [6] O. Toma, Chalcogenide Letters **8**(9), 541 (2011).
- [7] P. Roy, Thin Solid Films. **515**, 1912 (2006).
- [8] H Mamedov, Photonics Letters of Poland **10** (3), 73 (2015).
- [9] H. Mamedov, J. Optoelectron. Adv. M. **20** (9-10), 468 (2016).
- [10] V. Tregulov, Semiconductors **52**(7), 891 (2018).

*Corresponding author: maarif.jafarov@mail.ru